Materials Letters 169 (2016) 62–64

Contents lists available at ScienceDirect

Materials Letters

journal homepage: www.elsevier.com/locate/matlet

A multi-component $AlCrFe_2Ni_2$ alloy with excellent mechanical properties

Yong Dong, Xiaoxia Gao, Yiping Lu*, Tongmin Wang, Tingju Li

Key Laboratory of Solidification Control and Digital Preparation Technology (Liaoning Province), School of Materials Science and Engineering, Dalian University of Technology, Dalian 116024, China

ARTICLE INFO

Article history:
Received 16 November 2015
Received in revised form
14 December 2015
Accepted 20 January 2016
Available online 21 January 2016

Keywords:
High entropy alloys
Alloy design
Microstructure
Mechanical properties

ABSTRACT

A cost effective Co-free $AlCrFe_2Ni_2$ high entropy alloy was designed and prepared based on reported $AlCoCrFeNi_{2.1}$ eutectic high entropy alloys. The as-cast $AlCrFe_2Ni_2$ alloy showed a tensile yield strength of 796 MPa, an ultimate strength of 1437 MPa, and an elongation of 15.7%, which was superior to most high entropy alloys and was even comparable with the Ti-based ultrafine-grain alloy. The alloy consisted of noodle-like FCC phases, disordered BCC (A2) phases, and ordered BCC (B2) phases. The excellent mechanical properties of the alloy were attributed to the spinodal decomposition of BCC phases and the composite effect of the softer FCC and harder BCC phases.

1. Introduction

Recently, a new alloy category, called high entropy alloys (HEAs) [1] or multi-component alloys (MCAs) [2], was proposed by Yeh et al. and Cantor et al. The HEAs generally include at least five principal elements with the concentrations of each element being between 5 and 35 at% [1]. Special physical, chemical, and mechanical properties in HEAs have been reported [3–10]. According to the previous studies, single phase as-cast HEAs with a FCC structure usually have high plasticity but low tensile strength [11,12] while single phase as-cast HEAs with a BCC structure exhibit low plasticity [13]. To achieve a balance of strength, ductility, and castability, Lu et al. [5] proposed a composite method that uses the eutectic alloy idea to design HEAs with a mixture of FCC and BCC phases. Based on this design concept, an $AlCoCrFeNi_{2.1}$ eutectic HEA (EHEA) was designed and prepared. The casting alloy showed excellent mechanical properties with a fracture tensile stress of 944 MPa and an elongation of 25.6%. To reduce the cost and further improve the mechanical properties, in this paper, we tried to substitute equimole cheap Fe for the expensive Co and reduce the Ni element. Then, the new $AlCrFe_2Ni_2$ alloy was designed based on the $AlCoCrFeNi_{2.1}$ EHEA. The valence electron concentration (VEC) value of the new $AlCrFe_2Ni_2$ alloy is 7.5. According to the theory of Guo et al. [14], the new alloy should still have a FCC/BCC mixed structure.

2. Experimental details

The purity of all the raw elemental metals was above 99.9 wt%. Master ingots (105 g) with a nominal composition of $AlCrFe_2Ni_2$ were synthesized with a vacuum high-frequency induction melting furnace. After the vacuum pressure reached 3×10^{-3} Pa, melting and casting were performed with the pressure of 0.01 atm by backfilled to argon (Ar). The melting alloy was poured into a graphite crucible with a length of 80 mm, an upper inner diameter of 15 mm, and a bottom inner diameter of 12 mm. Dog-bone shaped specimens with gauge dimensions of 3 mm in diameter and 15 mm in length for use in tensile tests were taking from cylindrical casting ingot by electro-spark wire-electrode cutting and lathe machining. Prior to testing, the specimens were carefully mechanical ground and polished. The tensile tests were carried out on a UTM5105X universal electronic tensile testing machine with an initial strain rate of 10^{-3} s^{-1}. Three tensile measurements were employed for the reproducibility of the data. The cylindrical ingot was ground, polished, and etched with aqua regia for examining microstructures under an optical microscope (MEF-4) and a field-emission-gun scanning electron microscope (SEM, Zeiss supra 55) with energy dispersive spectrometry (EDS). Crystal structures were identified using an X-ray diffractometer (XRD, EMPYREAN with Cu radiation target) with the 2θ scan from 20° to 100°. Thin-foil specimens were prepared by mechanical thinning followed by ion milling and were observed under a transmission electron microscopy (TEM, Tecnai G220 S-Twin).

* Corresponding author.
E-mail address: luyiping@dlut.edu.cn (Y. Lu).

http://dx.doi.org/10.1016/j.matlet.2016.01.096
0167-577X/

3. Results and discussion

Fig. 1a shows the metallograph of the as-cast $AlCrFe_2Ni_2$ alloy. Typical grains with distinct grain boundaries were observed. However, there is a clear phase separation within the grains, where a large amount of noodle-like phases form and exist in disorder. Fig. 1b shows the high-magnified SEM secondary electron image. It can be seen that besides the noodle-like phases (denoted as A), bright and dark sections of interconnected microstructures (denoted as B) were also observed, which is a typical characteristic of spinodal decomposition [6,8]. From the EDS results (Table 1), region A contains more Fe and Cr and region B more Al and Ni. Generally, more Fe, Cr, and Ni prior to form FCC phases while more Al and Ni prefers to form ordered BCC (B2) phases [5,8]. Fig. 1c shows the XRD pattern of the alloy. The alloy exhibits a mixture of FCC, disordered BCC and ordered B2 crystal structures. The modulated microstructure often shows overlapping disordered BCC (A2) and B2 Bragg reflections in the XRD analysis. This was observed in many HEAs [6,8]. Fig. 2 shows a bright-field TEM micrograph of the as-cast $AlCrFe_2Ni_2$ alloy. The selected-area's electron diffraction pattern confirms that the noodle-like phases have an FCC structure, and the spinodal phases exhibit a BCC structure. Based on the dark field image in Fig. S1 (see Supplementary materials), in the spinodal structures, the precipitated-like particles are disordered A2, and the inter-precipitate are ordered B2.

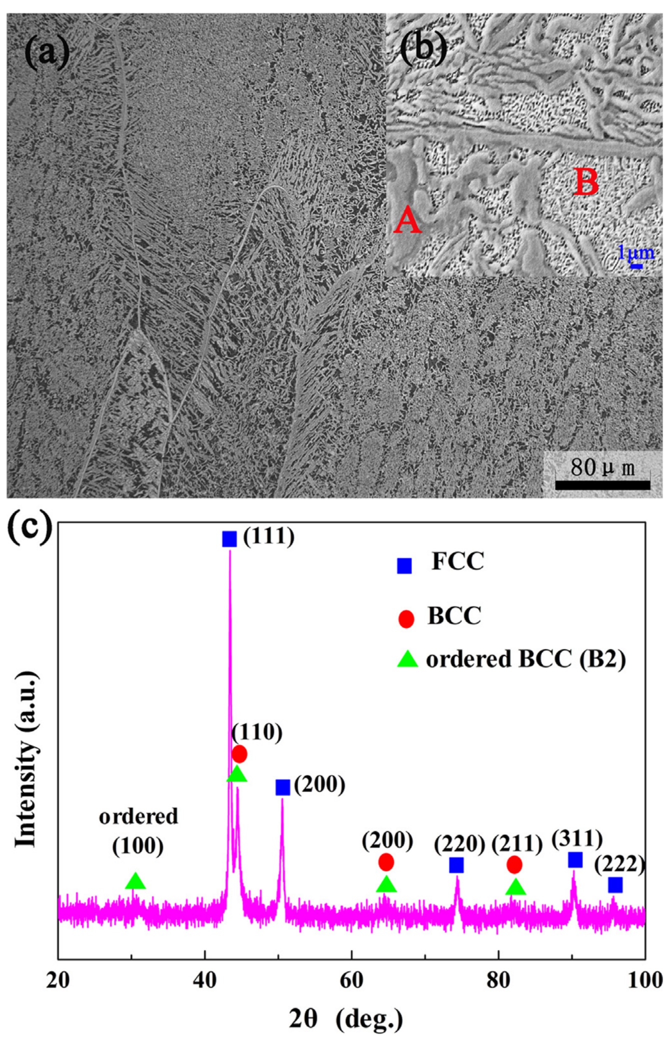

Fig. 1. Microstructure and crystal structure of as-cast $AlCrFe_2Ni_2$ alloy: (a) optical microscope photograph; (b) SEM secondary electron image; (c) XRD pattern.

Table 1
Chemical compositions of as-cast $AlCrFe_2Ni_2$ alloy by EDS (at%).

	Al	Cr	Fe	Ni
Nominal	16.7	16.7	33.3	33.3
Experimental	17.5	16.3	32.8	33.4
Region A	9.4	19.7	41.4	29.5
Region B	21.7	15.8	28.6	33.9

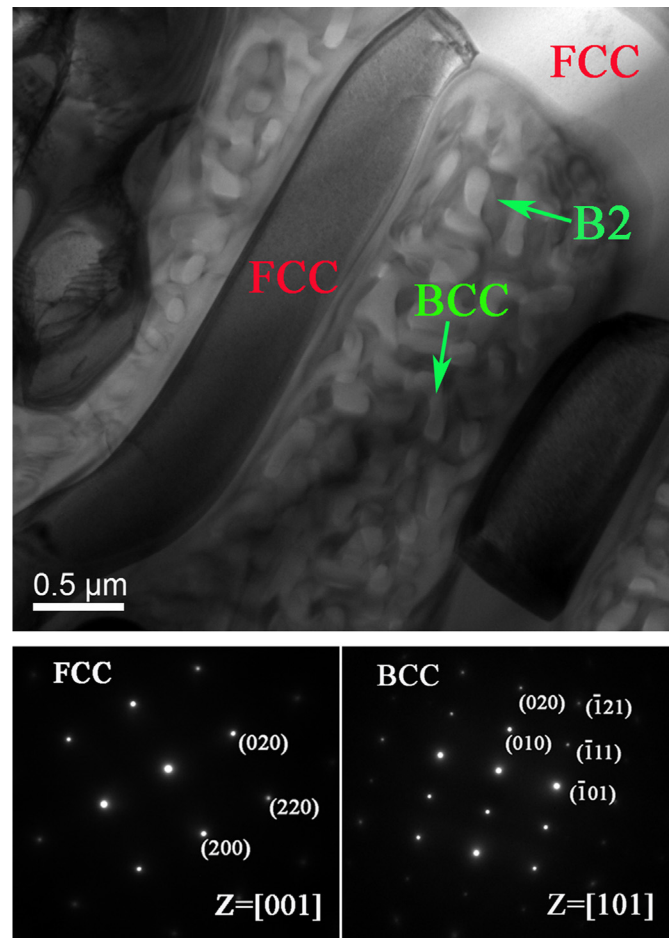

Fig. 2. Bright-field TEM image of as-cast $AlCrFe_2Ni_2$ alloy. The corresponding electron diffraction patterns of the [001] and [101] zone axis presented in the inset exhibit reflections of FCC and BCC, respectively.

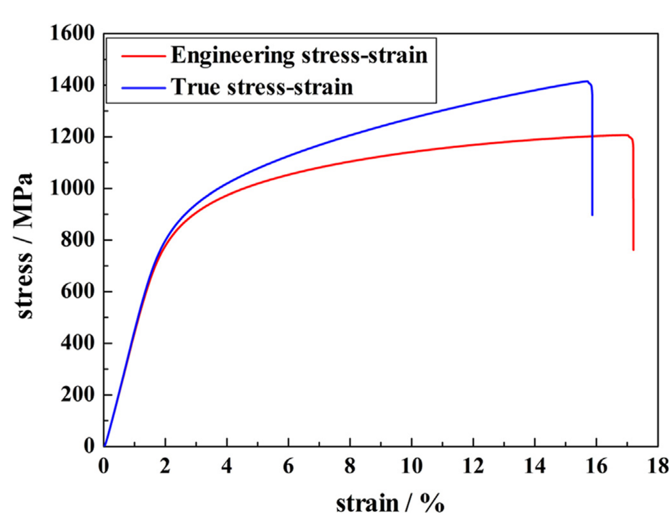

Fig. 3. Tensile stress-strain curve of as-cast $AlCrFe_2Ni_2$ alloy at room temperature.

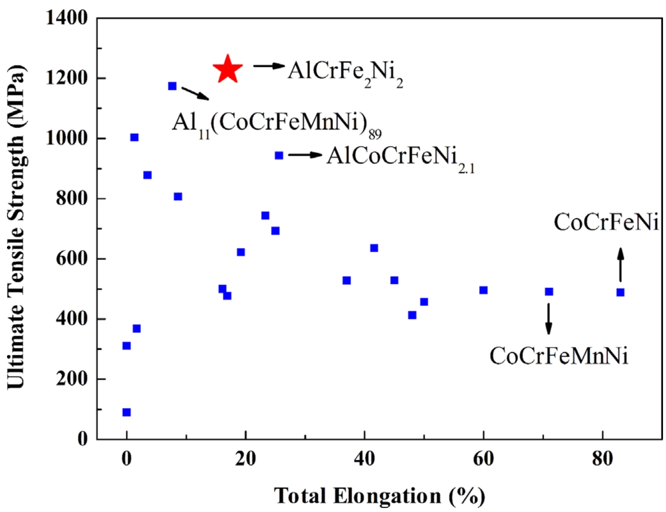

Fig. 4. Total elongation versus ultimate tensile strength for the reported as-cast HEAs in the engineering stress-strain condition.

Fig. 3 shows the stress-strain curves of the as-cast $AlCrFe_2Ni_2$ alloy. Surprisingly, the room temperature tensile tests showed that in the engineering stress-strain condition, the alloy has a yield strength of 780 MPa, an ultimate strength of 1228 MPa, and an elongation of 17%, respectively. These values were converted to 796 MPa, 1437 MPa, and 15.7% in the true stress-strain condition, respectively; this is comparable with Ti-based ultrafine-grain alloy [15]. It is extremely rare for an as-cast alloy to have such high strength and plasticity. Fig. 4 shows the total elongation versus ultimate tensile strength for the reported as-cast HEAs in the engineering stress-strain condition. The detailed tensile properties of some reported HEAs and titanium alloys are shown in Table S1 (see Supplementary materials). It is apparent that the mechanical properties of the as-cast $AlCrFe_2Ni_2$ alloy are superior to those of most titanium alloys at room temperature. In addition, the tensile fracture strength of the as-cast $AlCrFe_2Ni_2$ alloy is one of the highest among reported as-cast HEAs (see Fig. 4). Only a few HEAs in the as-rolled condition have a much larger ultimate tensile strength, but they sacrifice ductility [16].

The excellent mechanical properties of the as-cast $AlCrFe_2Ni_2$ alloy can be attributed to the spinodal decomposition of the BCC phases and the composite effect of the softer FCC and harder BCC phases [5]. Modulated microstructures with a mixture of A2 and B2 structures would lead to a high strength, similar to the high strength of the AlCoCrFeNi alloy [17]. In addition, the large volume fraction of softer noodle-like FCC phases could remedy the low ductility of the BCC phases, as seen in Fig. 1a and c.

4. Conclusion

In summary, we successfully designed a new $AlCrFe_2Ni_2$ alloy with an excellent combination of fracture strength and ductility. The new alloy is composed of the FCC and A2/B2 spinodal decomposition phases. The as-cast $AlCrFe_2Ni_2$ alloy shows a tensile yield strength of 796 MPa, an ultimate strength of 1437 MPa, and a total elongation of 15.7% in the true stress-strain condition. It is extremely rare for an as-cast alloy to have such high strength and plasticity. The mechanical properties of the $AlCrFe_2Ni_2$ alloy are superior to those of most titanium alloys and as-cast HEAs at room temperature.

Acknowledgments

This research was supported by the National Natural Science Foundation of China (Nos. 51104029, 51134013 and 51471044), the Fundamental Research Funds for the Central Universities, Key Laboratory of Basic Research Projects of Liaoning Province Department of Education (LZ2014007) and the Natural Science Foundation of Liaoning Province (2014028013).

Appendix A. Supporting information

Supplementary data associated with this article can be found in the online version at http://dx.doi.org/10.1016/j.matlet.2016.01.096.

References

[1] J.W. Yeh, S.K. Chen, S.J. Lin, J.Y. Gan, T.S. Chin, T.T. Shun, C.H. Tsau, S.Y. Chang, Adv. Eng. Mater. 6 (2004) 299–303.
[2] B. Cantor, I.T.H. Chang, P. Knight, A.J.B. Vincent, Mater. Sci. Eng. A 375–377 (2004) 213–218.
[3] B. Gludovatz, A. Hohenwarter, D. Catoor, E.H. Chang, E.P. George, R.O. Ritchie, Science 345 (2014) 1153–1158.
[4] Y. Zhang, T.T. Zuo, Z. Tang, M.C. Gao, K.A. Dahmen, P.K. Liaw, Z.P. Lu, Prog. Mater. Sci. 61 (2014) 1–93.
[5] Y.P. Lu, Y. Dong, S. Guo, L. Jiang, H.J. Kang, T.M. Wang, B. Wen, Z.J. Wang, J.C. Jie, Z.Q. Cao, H.H. Ruan, T.J. Li, Sci. Rep. 4 (2014) 6200.
[6] S. Singh, N. Wanderka, B.S. Murty, U. Glatzel, J. Banhart, Acta Mater. 59 (2011) 182–190.
[7] X.D. Xu, P. Liu, S. Guo, A. Hirata, T. Fujita, T.G. Nieh, C.T. Liu, M.W. Chen, Acta Mater. 84 (2015) 145–152.
[8] L.J. Santodonato, Y. Zhang, M. Feygenson, C.M. Parish, M.C. Gao, R.J.K. Weber, J. C. Neuefeind, Z. Tang, P.K. Liaw, Nat. Commun. 6 (2015) 5964.
[9] Y. Yu, J. Wang, J.S. Li, H.C. Kou, W.M. Liu, Mater. Lett. 138 (2015) 78–80.
[10] Y. Dong, Y.P. Lu, J.R. Kong, J.J. Zhang, T.J. Li, J. Alloy. Compd. 573 (2013) 96–101.
[11] W.H. Liu, J.Y. He, H.L. Huang, H. Wang, Z.P. Lu, C.T. Liu, Intermetalics 60 (2015) 1–8.
[12] J.Y. He, W.H. Liu, H. Wang, Y. Wu, X.J. Liu, T.G. Nieh, Z.P. Lu, Acta Mater. 62 (2014) 105–113.
[13] O.N. Senkov, G.B. Wilks, J.M. Scott, D.B. Miracle, Intermetallics 19 (2011) 698–706.
[14] S. Guo, C. Ng, J. Lu, C.T. Liu, J. Appl. Phys. 109 (2011) 103505.
[15] B.B. Sun, M.L. Sui, Y.M. Wang, G. He, J. Eckert, E. Ma, Acta Mater. 54 (2006) 1349–1357.
[16] N. Stepanov, M. Tikhonovsky, N. Yurchenko, D. Zyabkin, M. Klimova, S. Zherebtson, A. Efimov, G. Salishchev, Intermetallics 59 (2015) 8–17.
[17] Y.J. Zhou, Y. Zhang, Y.L. Wang, G.L. Chen, Appl. Phys. Lett. 90 (2007) 181904.